Quantum pumping and rectification effects in Aharonov-Bohm-Casher ring-dot systems

F. Romeo, R. Citro, and M. Marinaro
Dipartimento di Fisica "E. R. Caianiello," C.N.I.S.M. and NANOMATES (Research Centre for Nanomaterials and Nanotechnology), Università degli Studi di Salerno, Via S. Allende, I-84081 Baronissi (Sa), Italy

(Received 25 September 2008; revised manuscript received 7 November 2008; published 9 December 2008)

Within the nonequilibrium Green's-function formalism we study the time-dependent transport of charge and spin through a ring-shaped region sequentially coupled to a weakly interacting quantum dot in the presence of an Aharonov-Bohm flux and spin-orbit interaction. The time-dependent modulation of the spin-orbit interaction or of the corresponding Aharonov-Casher flux, together with the modulation of the dot level, induces an electrically pumped spin current at zero bias even in the absence of a charge current. The results beyond the adiabatic regime show that an additional rectification current with an anomalous current-phase relation is generated. We discuss the relevance of such term in connection with recent experiments on out-of-equilibrium quantum dots.

DOI: 10.1103/PhysRevB.78.245309 PACS number(s): 72.25.−b, 71.70.Ej, 85.35.−p

I. INTRODUCTION

In recent years the process of miniaturization of manmade electronic circuits has permitted to reach the molecular scale providing the opportunity of testing quantum mechanics in nanoelectronics measurements.[1] In this framework, one of the most exciting challenges is to encode information by means of the electron spin instead of the charge, giving rise to the so-called spin-based electronics or spintronics.[2,3] To face the need of spin-polarizing systems acting as a source in spintronics devices, one promising possibility is to exploit the quantum interference effects by external electric or magnetic fields. In ring-shaped structures made of semiconducting materials a spin-sensitive phase, the Aharonov-Casher phase,[4] is originated by the Rashba spin-orbit interaction.[5,6] Such phase combined with the Aharonov-Bohm phase[7] induced by a magnetic field is a useful tool to achieve spin-polarizing devices.[8,9] Another interesting phase interference effect is originated by the periodic modulation of two out-of-phase parameters affecting the scattering properties of a nanostructure. Such phase effect, known in the literature as quantum pumping, was first introduced by Thouless.[10] After the Thouless theory, a scattering approach to the adiabatic quantum pumping was formulated by Brouwer[11] who showed that the dc current pumped by means of an adiabatic modulation of two out-of-phase independent parameters can be expressed in terms of the parametric derivatives of the scattering matrix. In the adiabatic regime described by the Brouwer formula, i.e., when the pumping frequency is much slower than the tunneling rates, a dc current proportional to $\omega \sin(\varphi)$ is originated, with φ being the phase difference between the two parameters. Such theoretical prediction was verified experimentally by Switkes *et al.*[12] even though some anomalies in the current-phase relation have been reported. In particular, it has been observed a nonvanishing current at $\varphi=0$. Several anomalies observed in the experiment can be explained by rectification of ac displacement currents as proposed in Ref. 13. According to this work, the rectified currents are responsible for measurable effects which may be dominant over the pumping currents. In order to discriminate between rectified currents and pumping effects symmetry arguments can be exploited. For instance in the noninteracting case, the dc rectification voltage $V_{\rm rect}$ is symmetric under reversal of the magnetic field $V_{\rm rect}(B)=V_{\rm rect}(-B)$, while the voltage generated by a quantum pump is not. On the other hand, it has been shown in Ref. 14 that finite frequency effects, considered within a nonequilibrium Green's-function approach, can lead to current-phase relations of the form $I_c \sim a\sin(\varphi)+b\cos(\varphi)$, where the coefficients a and b are functions of the pumping frequency ω. Differently from the adiabatic regime where the pumped currents are odd function of the relative phase φ between the modulated parameters, in the general nonequilibrium case an indefinite parity could be expected.

In the following we analyze the charge and spin pumping in a ring-shaped conductor sequentially coupled to a quantum dot (see Fig. 1) and apply the nonequilibrium Green's-function approach to analyze the dc current from the adiabatic to nonadiabatic regime addressing the question about the existence of rectification terms. In the ring region shown in Fig. 1 the electrons feel an Aharonov-Bohm phase to-

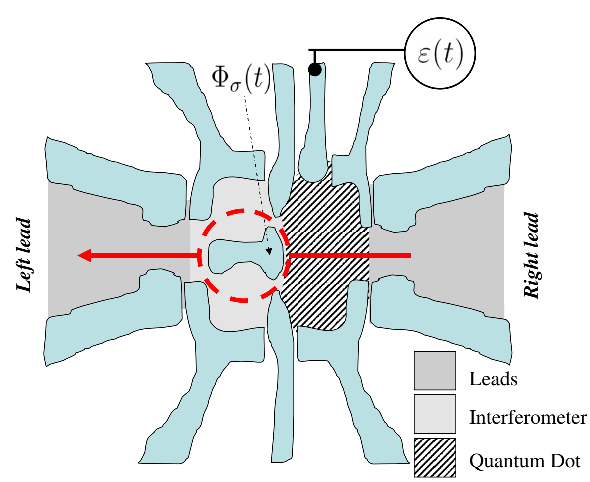

FIG. 1. (Color online) An Aharonov-Bohm-Casher quantum ring sequentially coupled to a quantum dot. The energy on the dot and the Aharonov-Casher flux are modulated in time with frequency ω.

1098-0121/2008/78(24)/245309(9)

gether with a time-varying Aharonov-Casher phase. The last is related to the Rashba spin-orbit interaction which is tunable by means of a gate voltage.[15] An additional time-dependent modulation of the dot energy level is also considered. If no voltage bias is present between the two external leads, the electron current is activated by absorption and emission of quantized photon energy. Thus, in the following the charge and spin-pumped currents are studied as a side effect of boson-assisted tunneling.

The paper is organized as follows. In Sec. II we introduce the model Hamiltonian and derive the general expression for the nonequilibrium Green's function and respective self-energies for the noninteracting and weakly interacting case. In Sec. III, we employ a one-photon-approximation and obtain a compact expression for the dc current pumped in the left lead. In Sec. IV, we present the results of our analysis as a function of the phase and interaction effects. Finally, in Sec. V some conclusions are given.

II. MODEL AND NONEQUILIBRIUM CURRENT

The Hamiltonian of an Aharonov-Bohm-Casher ring sequentially coupled to an interacting quantum dot in the presence of time-varying parameters can be written, in the local spin frame, as follows:[16]

$$H(t) = H_c + \sum_{\sigma} \varepsilon(t) d_\sigma^\dagger d_\sigma + U n_\uparrow n_\downarrow + \sum_{k\sigma} \{2u \cos[\Phi_\sigma(t)] d_\sigma^\dagger c_{k\sigma l} + w c_{k\sigma r}^\dagger d_\sigma\} + \text{H.c.}, \tag{1}$$

where $H_c=\sum_{k\sigma,\alpha=\{l,r\}}\varepsilon_k^\alpha c_{k\sigma\alpha}^\dagger c_{k\sigma\alpha}$ is the free-electron Hamiltonian describing the left/right (l/r) leads kept at the same chemical potential μ. The second and third term represent the dot Hamiltonian consisting of the electron-electron interaction term $Un_\uparrow n_\downarrow$ $(n_\sigma=d_\sigma^\dagger d_\sigma)$ and of the time-dependent dot energy level $\varepsilon(t)=\varepsilon_0+\varepsilon_\omega \sin(\omega t+\varphi)$, with ω being the frequency of the modulation. The last term in Hamiltonian describes the tunneling between the left lead and the dot, $u \cos(\Phi_\sigma)$, and the right lead and the dot through a tunnel barrier, w. The transmission coefficients u and w, which in general may be spin and momentum dependent, are considered here constant for simplicity, i.e., $u\approx u(k=k_F)$ and $w \approx w(k=k_F)$, with k_F being the Fermi momentum.

The electrons coming from the left lead acquire the time-dependent spin-sensitive phase $\Phi_\sigma(t)=\pi[\Phi_{\text{AB}}+\sigma\Phi_R(t)]$ $(\sigma=\pm1)$, where Φ_{AB} is the Aharonov-Bohm phase, while Φ_R is the Aharonov-Casher phase produced by the modulation of the Rashba spin-orbit interaction on the ring $\Phi_R(t)=\Phi_R^0+\Phi_R^\omega \sin(\omega t)$.[9] The Hamiltonian given in Eq. (1) can be rewritten by means of a plane-wave expansion in the following form:

$$H(t) = H_0 + \varepsilon_\omega \sin(\omega t+\varphi)\sum_\sigma d_\sigma^\dagger d_\sigma + \sum_{k\sigma} 4u[\cos(\Phi_\sigma^0)\mathcal{A}(\Phi_R^\omega,t) - \sigma \sin(\Phi_\sigma^0)\mathcal{B}(\Phi_R^\omega,t)] d_\sigma^\dagger c_{k\sigma l} + \text{H.c.}, \tag{2}$$

where the static part H_0 of the Hamiltonian is the same as in Eq. (1) with: $\varepsilon(t)\to\varepsilon_0$, $u\to uJ_0(\pi\Phi_R^\omega)$, $\Phi_R(t)\to\Phi_R^0$, and $\Phi_\sigma^0=\pi(\Phi_{\text{AB}}+\sigma\Phi_R^0)$, while the functions $\mathcal{A}(\Phi_R^\omega,t)$ and $\mathcal{B}(\Phi_R^\omega,t)$ are given by[17]

$$\mathcal{A}(\Phi_R^\omega,t) = \sum_{n=1}^\infty J_{2n}(\pi\Phi_R^\omega)\cos(2n\omega t), \tag{3}$$

$$\mathcal{B}(\Phi_R^\omega,t) = \sum_{n=1}^\infty J_{2n-1}(\pi\Phi_R^\omega)\sin[(2n-1)\omega t], \tag{4}$$

where $J_n(x)$ are the Bessel functions of first kind. In absence of an external voltage, the quantum transport of particles through the structure is only due to absorption or emission of energy quanta $\hbar\omega$ associated to the external time-dependent fields.

To calculate the pumped current we employ the Keldysh Green's-functions technique as formulated in Ref. 18. The current in the left lead is given by $I_l(t)=-e\frac{d}{dt}\langle N_l\rangle =-\frac{ie}{\hbar}\langle[H,N_l]\rangle$ $(N_l=\sum_{k\sigma}c_{k\sigma l}^\dagger c_{k\sigma l})$. It can be rewritten in terms of the retarded and lesser Green's functions $G_{\sigma\sigma'}^{r/<}(t,t_1)$ and of the advanced and lesser self-energies $\Sigma_{l,\sigma\sigma'}^{a/<}(t_1,t)$ of the quantum dot according to the following expression:

$$I_l(t) = \sum_\sigma I_l^\sigma(t), \tag{5}$$

$$I_l^\sigma(t) = \frac{2e}{\hbar}\sum_{\sigma'} Re\left\{\int dt_1 G_{\sigma\sigma'}^r(t,t_1)\Sigma_{l,\sigma'\sigma}^<(t_1,t) + G_{\sigma\sigma'}^<(t,t_1)\Sigma_{l,\sigma'\sigma}^a(t_1,t)\right\}. \tag{6}$$

For a time-dependent problem the retarded, advanced and lesser $(r,a,<)$ Green's functions and respective self-energies depend explicitly on two time variables instead of one. Thus, employing the two time Fourier transform[19] the current [Eq. (5)] can be rewritten as

$$I_l^\sigma(t) = \frac{2e}{\hbar}\sum_{\sigma'} Re\left\{\int \frac{dE_1dE_2dE_3}{(2\pi)^3}e^{i(E_3-E_1)t} \times [G_{\sigma\sigma'}^r(E_1,E_2)\Sigma_{l,\sigma'\sigma}^<(E_2,E_3) + G_{\sigma\sigma'}^<(E_1,E_2)\Sigma_{l,\sigma'\sigma}^a(E_2,E_3)]\right\}, \tag{7}$$

where the lesser Green's function $\mathbf{G}^<(E_1,E_2)$ of the dot is given by the Keldysh equation,

$$\mathbf{G}^<(E_1,E_2) = \int \frac{d\xi_1 d\xi_2}{(2\pi)^2}\mathbf{G}^r(E_1,\xi_1)\Sigma^<(\xi_1,\xi_2)\mathbf{G}^a(\xi_2,E_2), \tag{8}$$

and the following relation between the retarded and advanced quantities can be used: $\Xi^a(E_1,E_2)=[\Xi^r(E_2,E_1)]^\dagger$, where $\Xi=G$ or Σ. In order to compute the current the knowledge of G^r, Σ^r, and $\Sigma^<$ is required. Below we are going to calculate them for the noninteracting dot and the weakly interacting one. In both cases, the wide-band limit (WBL) will be employed for simplicity.

A. Noninteracting case ($U=0$)

In the $U=0$ case the expression of the self-energies can be obtained exactly. By calling $w=\gamma u$ $(\gamma\in\mathbf{R})$, the retarded and lesser self-energies can be expressed in terms of the corresponding Green's functions of the leads, namely, $[g^r_{k\alpha}(t,t')]_{sp}=-i\delta_{sp}\theta(t-t')e^{-i\varepsilon^\alpha_k(t-t')}$ and $[g^<_{k\alpha}(t,t')]_{sp}=i\delta_{sp}f(\varepsilon^\alpha_k)e^{-i\varepsilon^\alpha_k(t-t')}$, by the following relations:

$$\Sigma^{r,<}_{sp}(t_1,t_2)=\sum_{k,\alpha\in r}\gamma^2|u|^2[g^{r,<}_{kr}(t_1,t_2)]_{sp}+\sum_{k,\alpha\in l}4|u|^2\cos[\Phi_s(t_1)]\cos[\Phi_p(t_2)][g^{r,<}_{kl}(t_1,t_2)]_{sp},\tag{9}$$

where s,p are spin indices $(\uparrow,\downarrow)$ and $f(\varepsilon_k)$ is the Fermi function, while $\varepsilon^l_k=\varepsilon^r_k=\varepsilon_k$ in absence of voltage bias. In WBL limit and making the substitution $\Sigma_{k,\alpha}\to\int d\varepsilon\rho_\alpha(\varepsilon)$, we get

$$\Sigma^r_{sp}(t_1,t_2)=-i\delta_{sp}\delta(t_1-t_2)\Gamma^0\{\gamma^2/2+2\cos^2[\Phi_s(t_1)]\},$$

$$\Sigma^<_{sp}(t_1,t_2)\approx i\delta_{sp}f(t_1-t_2)\Gamma^0[\gamma^2+4\cos^2(\Phi_s(t_1))],\tag{10}$$

where we introduced the quantities $\Gamma^0=2\pi\rho|u|^2$ and $f(t_1-t_2)=\int\frac{d\varepsilon}{2\pi}f(\varepsilon)e^{-i\varepsilon(t_1-t_2)}$. By defining the left and right transition rates $\Gamma^l_s(t_1)/2=2\Gamma^0\cos^2[\Phi_s(t_1)]$ and $\Gamma^r_s(t_1)/2=\Gamma^0\gamma^2/2$, the retarded self-energy can be written as $\Sigma^r_{sp}(t_1,t_2)=-i\delta_{sp}\delta(t_1-t_2)\{\Gamma^l_s(t_1)/2+\Gamma^r_s(t_1)/2\}$ and thus the retarded Green's function of the quantum dot takes the following form:[20]

$$G^r_{sp}(t,t')=g^r_{sp}(t,t')\exp\left\{-\frac{1}{2}\int_{t'}^{t}dt_1[\Gamma^l_s(t_1)+\Gamma^r_s(t_1)]\right\},$$

$$g^r_{sp}(t,t')=-i\delta_{sp}\theta(t-t')\exp\left\{-i\int_{t'}^{t}dt_1\varepsilon(t_1)\right\}.\tag{11}$$

It can be computed exactly after having performed the following plane-wave expansion of the retarded self-energy:

$$\begin{aligned}\Sigma^r_{sp}(t_1,t_2)=&-i\delta_{sp}\delta(t_1-t_2)\Gamma^0[1+\gamma^2/2+J_0(2\pi\Phi^\omega_R)\cos(2\Phi^0_s)\\&+2\cos(2\Phi^0_s)\mathcal{A}(2\Phi^\omega_R,t_1)\\&-2s\sin(2\Phi^0_s)\mathcal{B}(2\Phi^\omega_R,t_1)],\end{aligned}\tag{12}$$

whose Fourier transform is given by

$$\begin{aligned}\Sigma^r_{sp}(E_1,E_2)&\\=-\pi\delta_{sp}\Bigg\{&i\delta(E_1-E_2)\mathcal{Q}^s_1+i\mathcal{Q}^s_2\\&\times\sum_{\eta=\pm1,n=1}^{\infty}J_{2n}(2\pi\Phi^\omega_R)\delta(E_1-E_2+2n\omega\eta)-\mathcal{Q}^s_3\\&\times\sum_{\eta=\pm1,n=1}^{\infty}\eta J_{2n-1}(2\pi\Phi^\omega_R)\delta[E_1-E_2+(2n-1)\omega\eta]\Bigg\}.\end{aligned}\tag{13}$$

An analogous plane-wave expansion can be performed for the lesser self-energy $\Sigma^<_{sp}(t_1,t_2)$, whose Fourier transform is the following:

$$\begin{aligned}\Sigma^<_{sp}(E_1,E_2)&\\=2\pi i\delta_{sp}\Bigg\{&f(E_1)\delta(E_1-E_2)\mathcal{Q}^s_1+\sum_{\eta=\pm1,n=1}^{\infty}\mathcal{Q}^s_2J_{2n}(2\pi\Phi^\omega_R)\\&\times f(E_1+2n\omega\eta)\delta(E_1-E_2+2n\omega\eta)\\&+\sum_{\eta=\pm1,n=1}^{\infty}i\mathcal{Q}^s_3\eta J_{2n-1}(2\pi\Phi^\omega_R)f[E_1+(2n-1)\omega\eta]\\&\times\delta(E_1-E_2+(2n-1)\omega\eta)\Bigg\},\end{aligned}\tag{14}$$

where $\mathcal{Q}^s_j$ are given by

$$\mathcal{Q}^s_1=2\Gamma^0\{\gamma^2/2+1+J_0(2\pi\Phi^\omega_R)\cos(2\Phi^0_s)\},$$

$$\mathcal{Q}^s_2=2\Gamma^0\cos(2\Phi^0_s),$$

$$\mathcal{Q}^s_3=2\Gamma^0 s\sin(2\Phi^0_s).\tag{15}$$

The substitution of Eq. (14) and of $\mathbf{G}^r(E_1,E_2)$ in Eq. (8) permits to determine the $\mathbf{G}^<(E_1,E_2)$.

The knowledge of the retarded and lesser Green's function enables us to calculate the current generated by the pumping procedure in the form of a trigonometric series, i.e., $I^\sigma_l(t)=I^\sigma_0+\Sigma^\infty_{n=1}[c^\sigma_n\cos(n\omega t)+s^\sigma_n\sin(n\omega t)]$, allowing us to recognize the dc component of the current.

The self-energy plane-wave expansion above [Eq. (12)] applies to the adiabatic as well as to the antiadiabatic regime. When limiting the analysis to the adiabatic regime only, an expansion to the linear order in the time derivative or an average time approximation as in Ref. 21 can be employed.

B. Weakly interacting case ($U\approx0$)

The weakly interacting limit $(U\approx0)$ can be studied by means of a self-consistent Hartree-Fock theory which is known to give suitable results when the Coulomb interaction U is small (i.e., $U\ll\Gamma^0$).[22,23] In this framework, the energy of the electrons on the dot is modified by a spin-dependent term related to the occupation number of the electron of opposite spin and thus the spin-dependent energy becomes $\varepsilon_\sigma(t)=\varepsilon(t)+U\langle n_{\bar\sigma}(t)\rangle$ $(\bar\sigma=-\sigma)$. The occupation number $\langle n_\sigma(t)\rangle$ is calculated self-consistently by means of the relation $i\langle n_\sigma(t)\rangle=G^<_{\sigma\sigma}(t,t)$. Furthermore, the retarded Green's function of the dot is modified by the interaction according to the expression,

$$\mathcal{G}^r_{sp}(t,t') = G^r_{sp}(t,t')\exp\left\{-iU\int_{t'}^{t} dt_1 \langle n_{\bar{s}}(t_1)\rangle\right\}, \quad (16)$$

where $G^r_{sp}(t,t')$ represents the retarded Green's function derived in the noninteracting case. In order to determine the interacting Green's function, we can write $\langle n_{\bar{s}}(t_1)\rangle$ as a trigonometric series of $\sin(n\omega t)$ and $\cos(n\omega t)$ with unknown coefficients calculated in a self-consistent way, as explained below.

III. SINGLE-PHOTON APPROXIMATION

Hereon we focus on the weak pumping limit and consider only single-photon processes, i.e., involving emission or absorption of a single energy quantum $\hbar\omega$. The weak pumping limit [i.e., the case in which a pure $\sin(\varphi)$ behavior of the current is expected] is very important in experiments where the higher harmonics contribution seem to be negligible even though other anomalies occur. Such anomalies in the current-phase relation will be discussed here later.

A. Noninteracting case ($U=0$)

Within the single-photon approximation the self-energies [Eqs. (13) and (14)] can be approximated as

$$\Sigma^r_{sp}(E_1,E_2) \approx -\pi\delta_{sp}\left\{i\delta(E_1-E_2)\mathcal{Q}^s_1 + \mathcal{Q}^s_3 J_1(2\pi\Phi^\omega_R) \times \sum_{\eta=\pm1}\eta\delta(E_1-E_2-\eta\omega)\right\},$$

$$\Sigma^<_{sp}(E_1,E_2) \approx 2\pi\delta_{sp}\left\{if(E_1)\mathcal{Q}^s_1 - \mathcal{Q}^s_3 J_1(2\pi\Phi^\omega_R) \times \sum_{\eta=\pm1}\eta f(E_1+\eta\omega)\delta(E_1-E_2+\eta\omega)\right\}. \quad (17)$$

The approximation is valid for small values of $2\pi\Phi^\omega_R$ so that the inequality $J_1(2\pi\Phi^\omega_R) \gg J_n(2\pi\Phi^\omega_R)$, $n>1$, is verified. Using the above approximated form of Eq. (17) the retarded Green's function of the quantum dot can be rewritten as follows:

$$G^{r(1)}_{sp}(t,t') = -i\delta_{sp}\theta(t-t')\exp\{-i[\varepsilon_0 - i\mathcal{Q}^s_1/2](t-t')\} \times\exp\left\{-i\left[\Lambda^s_1\int_{t'}^{t} dt_1 \sin(\omega t_1) + \Lambda_2\int_{t'}^{t} dt_1 \cos(\omega t_1)\right]\right\}, \quad (18)$$

where we introduced the coefficients,

$$\Lambda^s_1 = \varepsilon_\omega\cos(\varphi) + iJ_1(2\pi\Phi^\omega_R)\mathcal{Q}^s_3,$$

$$\Lambda_2 = \varepsilon_\omega \sin(\varphi), \quad (19)$$

and the upper index (1) stands for the single-photon approximation. Making a further expansion of the retarded Green's function for small $\varepsilon_\omega/\omega$ leads to the result,

$$G^{r(1)}_{sp}(t,t') \simeq -i\delta_{sp}\theta(t-t')\exp\{-i[\varepsilon_0 - i\mathcal{Q}^s_1/2](t-t')\} \times\{\Delta^s_0 + \Delta^s_1\mathcal{C}(t,t') + \Delta^s_2\mathcal{S}(t,t')\}, \quad (20)$$

where $\mathcal{C}(t,t')=\cos(\omega t')-\cos(\omega t)$ and $\mathcal{S}(t,t')=\sin(\omega t')-\sin(\omega t)$, while the coefficients Δ^s_j have been defined as follows:

$$\Delta^s_0 = J_0\left(\frac{\Lambda_2}{\omega}\right)^2 J_0\left(\frac{\mathrm{Re}\{\Lambda^s_1\}}{\omega}\right)^2 I_0\left(\frac{\mathrm{Im}\{\Lambda^s_1\}}{\omega}\right)^2,$$

$$\Delta^s_1 = 2J_0\left(\frac{\Lambda_2}{\omega}\right)^2 I_0\left(\frac{\mathrm{Im}\{\Lambda^s_1\}}{\omega}\right) J_0\left(\frac{\mathrm{Re}\{\Lambda^s_1\}}{\omega}\right) \times\left[J_0\left(\frac{\mathrm{Re}\{\Lambda^s_1\}}{\omega}\right) I_1\left(\frac{\mathrm{Im}\{\Lambda^s_1\}}{\omega}\right) - iJ_1\left(\frac{\mathrm{Re}\{\Lambda^s_1\}}{\omega}\right) \times I_0\left(\frac{\mathrm{Im}\{\Lambda^s_1\}}{\omega}\right)\right],$$

$$\Delta^s_2 = 2iI_0\left(\frac{\mathrm{Im}\{\Lambda^s_1\}}{\omega}\right)^2 J_0\left(\frac{\mathrm{Re}\{\Lambda^s_1\}}{\omega}\right)^2 J_1\left(\frac{\Lambda_2}{\omega}\right) J_0\left(\frac{\Lambda_2}{\omega}\right), \quad (21)$$

where $I_n(x)$ $(n=0,1)$ represents the modified Bessel function of first kind and order n. The above result can be conveniently rewritten in terms of the two-time Fourier transform, and thus we have

$$G^{r(1)}_{sp}(E_1,E_2) = 2\pi\delta_{sp}\left\{\frac{\Delta^s_0\delta(E_1-E_2)}{\mathcal{D}^s(E_1)} + \sum_{\eta=\pm1}\frac{\eta\omega\mathcal{R}^s_\eta\delta(E_1-E_2+\eta\omega)}{\mathcal{D}^s(E_1)[\mathcal{D}^s(E_1)+\eta\omega]}\right\}, \quad (22)$$

where we defined $\mathcal{R}^s_\eta=(\Delta^s_1 - i\eta\Delta^s_2)/2$ and $\mathcal{D}^s(E_1)=E_1-\varepsilon_0+i\mathcal{Q}^s_1/2$. The knowledge of the retarded Green's function allows us to write the lesser Green's function by means of the Keldysh equation in this way;

$$G^{<(1)}_{ss}(E_1,E_2) = 2\pi i\mathcal{Q}^s_1\mathcal{F}^0_s(E_1,E_2) + 2\pi\mathcal{Q}^s_3 J_1(2\pi\Phi^\omega_R)\sum_{\eta=\pm1}\eta\mathcal{F}^{-\eta}_s(E_1,E_2), \quad (23)$$

where we defined the following integral function:

$$\mathcal{F}^\eta_\sigma(E_1,E_2) = \sum_s\int\frac{d\xi}{(2\pi)^2}G^{r(1)}_{\sigma s}(E_1,\xi-\eta\omega) \times f(\xi)G^{r(1)*}_{\sigma s}(E_2,\xi). \quad (24)$$

The above function, disregarding terms quadratic in $J_1(x)$ and $I_1(x)$ and additional terms describing higher-order processes [roughly cubic in $\sim(\mathcal{D}^s(E_1))^{-1}$], can be written in the simple form,

$$\mathcal{F}_s^\eta(E_1,E_2) = \frac{f(E_1+\eta\omega)[\Delta_0^s]^2\delta(E_1-E_2+\eta\omega)}{\mathcal{D}^s(E_1)[\mathcal{D}^s(E_1)+\eta\omega]^*}. \quad (25)$$

Thus, the dc current generated by the time-varying parameters has the following final expression:

$$\langle I_l^{s(1)}(t)\rangle = \frac{e\tilde{\mathcal{Q}}_1^s\mathcal{Q}_1^s\Delta_0^s[1-\Delta_0^s]}{h}\int\frac{f(E)dE}{|\mathcal{D}^s(E)|^2} + \frac{2e\mathcal{Q}_3^sJ_1(2\pi\Phi_R^\omega)}{h} \times \mathrm{Re}\left\{\sum_{\eta=\pm1}\int\frac{\omega\mathcal{R}_\eta^s f(E)dE}{\mathcal{D}^s(E)[\mathcal{D}^s(E)+\eta\omega]}\right\}. \quad (26)$$

Here $\tilde{\mathcal{Q}}_1^s$ is a coefficient obtained setting $\gamma=0$ in $\mathcal{Q}_1^s$ (for the left lead). The current [Eq. (26)] contains terms proportional to ε_ω^2 and $(\Phi_R^\omega)^2$ that can be interpreted as rectification terms and terms proportional to $\varepsilon_\omega\Phi_R^\omega$ which contain information on the nonadiabatic pumping process, as will be clear below.

B. Weakly interacting case ($U\approx 0$)

To perform the analysis in the weakly interacting case, we consider U/ω as a small quantity, with U being of the same order of ε_ω and Φ_R^ω. This implies that terms proportional to $U\omega$ are negligible (i.e., $U\omega \ll \omega^2$). Within the Hartree-Fock theory we need to determine the energy of the quantum dot $\varepsilon_\sigma(t)=\varepsilon_0+Un_{\bar{\sigma}}(t)$ with $n_{\bar{\sigma}}(t)\equiv\langle n_{\bar{\sigma}}(t)\rangle$. By using the single-photon approximation, we write the occupation number as a trigonometric series,

$$n_\sigma(t) = a_\sigma^{(0)} + a_\sigma^{(1)}\sin(\omega t) + a_\sigma^{(2)}\cos(\omega t), \quad (27)$$

where the unknown coefficients $a_\sigma^{(i)}$ have to be determined self-consistently. In the interacting case the retarded Green's function takes the following form:

$$G_{sp}^{r(1)}(t,t') = -i\delta_{sp}\theta(t-t')\exp\{-i[\varepsilon_0+Ua_{\bar{s}}^{(0)}-i\mathcal{Q}_1^s/2] \times(t-t')\}\exp\left\{-i\left[(\Lambda_1^s+Ua_{\bar{s}}^{(1)})\int_{t'}^t dt_1\sin(\omega t_1) + (\Lambda_2+Ua_{\bar{s}}^{(2)})\int_{t'}^t dt_1\cos(\omega t_1)\right]\right\}. \quad (28)$$

Note that since the coefficients $a_s^{(i)}$ appear as a factor of the interaction U, we have to calculate them only up to the zero-order approximation in U and ω. From the lesser Green's function obtained by Eq. (28), we can write the occupation number in the following form:

$$n_\sigma(t) \approx \frac{(\Delta_0^\sigma)^2}{2\pi}[\mathcal{Q}_1^\sigma - 2\mathcal{Q}_3^\sigma J_1(2\pi\Phi_R^\omega)\sin(\omega t)]\int\frac{f(E)dE}{|\mathcal{D}_0^s(E)|^2}, \quad (29)$$

where $\mathcal{D}_0^\sigma(E)=E-\varepsilon_0+i\mathcal{Q}_1^s/2$. By comparing the above expression with the $G_{\sigma\sigma}^{<(1)}(t,t)$ obtained by using Eq. (28) one gets the following set of self-consistency equations:

$$a_\sigma^{(0)} = \frac{\mathcal{Q}_1^\sigma}{2\pi}\int\frac{f(E)dE}{|\mathcal{D}_0^\sigma(E)|^2},$$

$$a_\sigma^{(1)} = -2\frac{\mathcal{Q}_3^\sigma}{\mathcal{Q}_1^\sigma}J_1(2\pi\Phi_R^\omega)a_\sigma^{(0)},$$

$$a_\sigma^{(2)} = 0. \quad (30)$$

Once the above equations are solved, the dc current can be written as in Eq. (26) with the following interaction-induced shift:
$\varepsilon_0\rightarrow\varepsilon_0+Ua_{\bar{\sigma}}^{(0)}$ and $\Lambda_1^s\rightarrow\Lambda_1^s+Ua_{\bar{\sigma}}^{(1)}$.

C. Spin and charge currents

To obtain an analytical expression of the dc current pumped in the left lead in the presence of a weak interaction and zero temperature, we expand $\mathcal{R}_\eta^s$ in [Eq. (26)] for $\frac{\varepsilon_\omega}{\omega}\ll 1$ and $2\pi\Phi_R^\omega\ll 1$. In this limit the coefficients $\mathcal{R}_\eta^s$ reduce to

$$\mathcal{R}_\eta^s \approx \frac{\pi\Phi_R^\omega\mathcal{Q}_3^s}{2\omega} + \eta\frac{\varepsilon_\omega\sin(\varphi)}{2\omega} - i\frac{[\varepsilon_\omega\cos(\varphi)+Ua_{\bar{s}}^{(1)}]}{2\omega}, \quad (31)$$

while the quantity $\Delta_0^s[1-(\Delta_0^s)]$ can be written as follows:

$$\Delta_0^s[1-\Delta_0^s] \approx \frac{1}{2}\left[\frac{\varepsilon_\omega^2}{\omega^2} - \frac{(\pi\Phi_R^\omega\mathcal{Q}_3^s)^2}{\omega^2} + 2\frac{a_{\bar{s}}^{(1)}U\varepsilon_\omega\cos(\varphi)}{\omega^2}\right] + \mathcal{O}(1/\omega^4). \quad (32)$$

Plugging these expressions in Eq. (26) and performing the integral over the frequency, we can write the dc current in the single-photon approximation (in units of $2\Gamma^0 e/\hbar$) as follows:

$$\langle i_\sigma^{(1)}\rangle = \frac{\tilde{q}_1^\sigma a_\sigma^{(0)}}{2\omega^2}[\varepsilon_\omega^2 - (2\pi\Phi_R^\omega q_3^\sigma)^2 + 2a_{\bar{\sigma}}^{(1)}U\varepsilon_\omega\cos(\varphi)] + [-\pi(q_3^\sigma\Phi_R^\omega)^2]\left[\frac{\mu-\varepsilon_0+U(a_\sigma^{(0)}-a_{\bar{\sigma}}^{(0)})}{|\mathcal{D}^\sigma(\mu)|^2}\right] + q_3^\sigma\frac{\varepsilon_\omega\Phi_R^\omega}{2|\mathcal{D}^\sigma(\mu)|^2}\left\{\frac{\omega\sin(\varphi)}{|\mathcal{D}^\sigma(\mu)|^2}[(\mu-\varepsilon_0-Ua_{\bar{\sigma}}^{(0)})^2-(q_1^\sigma)^2] + 2q_1^\sigma\cos(\varphi)\right\} + \mathcal{O}(\omega^3), \quad (33)$$

where the energies are measured in units of Γ^0, while we defined $q_i^\sigma\equiv\mathcal{Q}_i^\sigma/(2\Gamma^0)$. The dimensionless charge and spin currents, i.e., I_c and I_s, can be defined as $I_c=\Sigma_\sigma i_\sigma$ and $I_s=\Sigma_\sigma\sigma i_\sigma$. The main feature of the expression for the dc current is the presence of a nonsinusoidal current-phase relation already in weak pumping. Indeed, contrarily to the adiabatic case characterized by a current-phase relation with odd parity [i.e., $I_c(-\varphi)=-I_c(\varphi)$] in the time-dependent case an indefinite parity could be expected. This behavior is mainly related to finite frequency effects as well as to interaction effects. Equation (33) represents the main result of this work.

IV. NUMERICAL RESULTS AND DISCUSSION

In order to make a comparison with the available experimental data, we set $\Gamma^0\sim 10\mu\mathrm{eV}$.[24] This quantity is related to

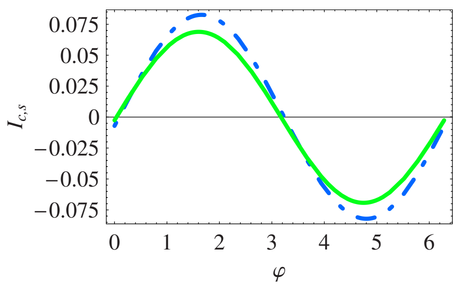

FIG. 2. (Color online) Currents of charge (dashed-dotted line) and spin (full line) as a function of φ obtained for the following choice of parameters: $\gamma=0.05$, $\Phi_{AB}=0.49$, $\Phi_R^0=0.02$, $\Phi_R^\omega=0.01$, $\varepsilon_0=0$, $\varepsilon_\omega=0.025$, $\omega=0.1$, and $U=0$.

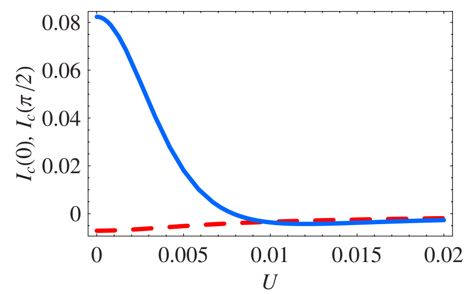

FIG. 3. (Color online) Currents of charge computed at: $\varphi=0$; $I_c(\varphi=0)$ (dashed line) and $\varphi=\pi/2$; $I_c(\varphi=\pi/2)$ (full line), as a function of U obtained for the following choice of parameters: $\gamma=0.05$, $\Phi_{AB}=0.49$, $\Phi_R^0=0.02$, $\Phi_R^\omega=0.01$, $\varepsilon_0=0$, $\varepsilon_\omega=0.025$, and $\omega=0.1$.

the dwell time τ_d by the following relation $E_\tau=h/\tau_d\sim 2\Gamma^0$, and it is relevant to define the various transport regimes at varying frequency ω. Indeed, for value of $\omega\tau_d \ll 1$ one deals with the adiabatic regime, while in the opposite limit, i.e., $\omega\tau_d \gg 1$, the nonadiabatic regime is approached. For typical experimental frequencies ranging from 10 MHz up to 20 GHz, $\omega\tau_d$ varies from $\sim 10^{-2}$ up to the order of 10 and thus the megahertz range of frequency can be safely considered as adiabatic. The dimensionless frequency ω which appears in Eq. (33) is defined as $\omega \equiv \hbar\omega/\Gamma^0=\omega\tau_d/\pi$. In this way a frequency of 25 MHz corresponds to $\omega=0.01$, 100 MHz corresponds to $\omega=0.04$, and 1 GHz corresponds to $\omega=0.4$. In the following we study the behavior of charge and spin currents in the range of frequency $\omega \in [0.1,0.5]$, thus our analysis is valid from adiabatic up to the moderate nonadiabatic limit. We also set the chemical potential μ as the zero of energy and consider the zero-temperature limit. From the analysis of the current i_σ, we notice the presence of two classes of terms contributing to the currents. (1) Terms proportional to ε_ω^2 or $(\Phi_R^\omega)^2$ and (2) terms proportional to $\Phi_R^\omega\varepsilon_\omega$. The first type of terms are nonadiabatic in nature. The second class of terms contains a term proportional to ω, which can be recognized as the quantum pumping contribution, and a frequency-independent term proportional to $\cos(\varphi)$ which can be interpreted as a rectification contribution. Such term is responsible for the nonsinusoidal behavior that leads to an anomalous current-phase relation as observed in Ref. 24 (page 3, first column, line 2). Very interestingly, the interaction effects also lead to a cosine term which is proportional to $a_{\bar{\sigma}}^{(1)}U\varepsilon_\omega\cos(\varphi)/\omega^2 \sim U\varepsilon_\omega\Phi_R^\omega\cos(\varphi)/\omega^2$ [see Eq. (33), first line]. Such a term produces a deviation from the sinusoidal behavior also for small values of the energy U. Finally, the current i_σ vanishes when the amplitude of the modulation ε_ω and Φ_R^ω go simultaneously to zero.

In Fig. 2 the charge (dashed-dotted line) and spin (full line) currents, namely, I_c and I_s, as a function of the phase difference φ between the time-varying parameters are reported for the following choice of parameters: $\gamma=0.05$, $\Phi_{AB}=0.49$, $\Phi_R^0=0.02$, $\Phi_R^\omega=0.01$, $\varepsilon_0=0$, $\varepsilon_\omega=0.025$, $\omega=0.1$, and $U=0$. A sinusoidal-like behavior is observed even though the charge pumped for $\varphi=0$ is different from zero and of the order of 10^{-3}. This is a fingerprint of the anomalous current-phase relation, as discussed above. To put in evidence the dependence on the interaction U, we present in Fig. 3 the charge current computed at $\varphi=0$ (dashed line) and $\varphi=\pi/2$ (full line) as a function of U taking the remaining parameters as in Fig. 2. Smaller values of the interaction favor deviation from the sinusoidal behavior.

Below we concentrate on the role of spin-orbit interaction and choose the Aharonov-Bohm flux close to half-integer values in unit of the flux quantum $\Phi_0=h/e$ where the charge current is activated by photon-assisted tunneling (PAT). Away from the above values of the Aharonov-Bohm flux the currents present an oscillating behavior as a function of the applied magnetic flux Φ_{AB} similar to the one already discussed in a previous work.[25]

In Fig. 4 we plot I_c (dashed-dotted line) and I_s (full line) as a function of the static Aharonov-Casher phase Φ_R^0 for pumping frequency $\omega=0.2$, $\omega=0.3$, and $\omega=0.4$ (from top to bottom) and by setting the remaining parameters as follows: $\gamma=0.05$, $\Phi_{AB}=0.49$, $\Phi_R^\omega=0.01$, $\varepsilon_0=-0.025$, $\varepsilon_\omega=0.05$, $\varphi=5\pi/4$, and $U=0$. By increasing the pumping frequency from $\omega=0.2$ (500 MHz) up to 0.4 (1 GHz) zeros of the charge currents start to appear and thus it is possible to obtain pure spin currents in the nonadiabatic regime. It is worth mentioning that currents of amplitude 10^{-2} in dimensionless units correspond to ~ 50 pA, thus the pure spin current we find is sizable.

To analyze the role of a weak Coulomb interaction, we plot in the upper panel of Fig. 5 the charge and spin currents for the same parameters as in Fig. 4 ($\omega=0.3$) and by setting $U=0.02$. A qualitatively different behavior of the charge current as a function of the Aharonov-Casher flux is observed. In particular, when the interaction energy U is of the same order of magnitude of the pumping frequency ω, additional zeros of the charge current appear and this is a very appealing situation for spintronics devices. For instance, looking at Fig. 5 (upper panel), one observes a pure spin current close to $\Phi_R^0=0.015$ and 0.03.

In the lower panel of Fig. 5 we plot charge and spin currents as done in the upper panel and by setting the Aharonov-Bohm flux to $\Phi_{AB}=0.52$. In this case, a characteristic oscillating behavior of the currents controlled by using a magnetic flux is visible.

Another interesting phenomenon is the asymmetric contribution to the current of the photon absorption and emission as a function of the dot level ε_0, as also reported in Ref. 26. When the dot level lies above the Fermi level ($\varepsilon_0>0$), an electron on the dot can jump in the left lead by emitting a

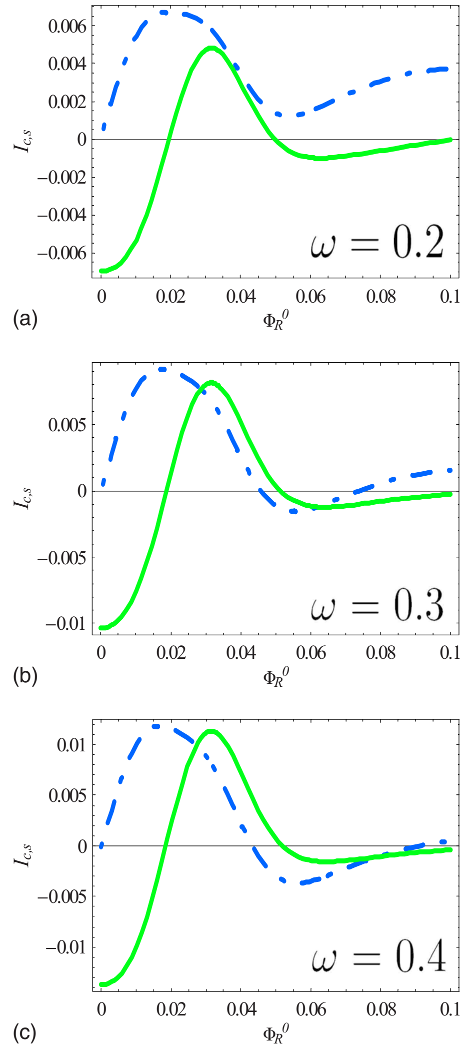

FIG. 4. (Color online) Charge (dashed-dotted line) and spin (full line) currents as a function of Φ_R^0 obtained for the following choice of parameters: γ=0.05, Φ_{AB}=0.49, Φ_R^ω=0.01, ε_0=−0.025, ε_ω=0.05, φ=5π/4, and U=0. The upper panel is obtained for ω=0.2, the middle panel for ω=0.3, and the lower panel for ω=0.4.

photon. For $\varepsilon_0<0$, an electron on the dot can reach the left lead only by means of the absorption of a photon since no voltage bias or temperature gradient is present. Because of the interference between these two-photon sources, boson-assisted tunneling onto the dot gets suppressed while tunneling out of the quantum dot is enhanced. The asymmetric behavior of the dc current as a function of the dot level is shown in Fig. 6.

In the upper panel, we plot the charge current I_c as a function of the dot level ε_0 and by setting the remaining parameters as γ=0.05, Φ_{AB}=0.49, Φ_R^0=0.05, Φ_R^ω=0.01, $\varphi=\pi/2$, U=0, and ε_ω=0.05. As can be seen, when the frequency ω is increased from 0.1 (dashed line) up to 0.5 (full line) a strong peak is formed at Fermi energy and the asymmetry of the current with respect to the ε_0=0 becomes more evident. It is worth to mention that since the relative phase φ is $\pi/2$, all the terms in the current proportional to cos(φ) are suppressed, while the pumping term takes its maximum

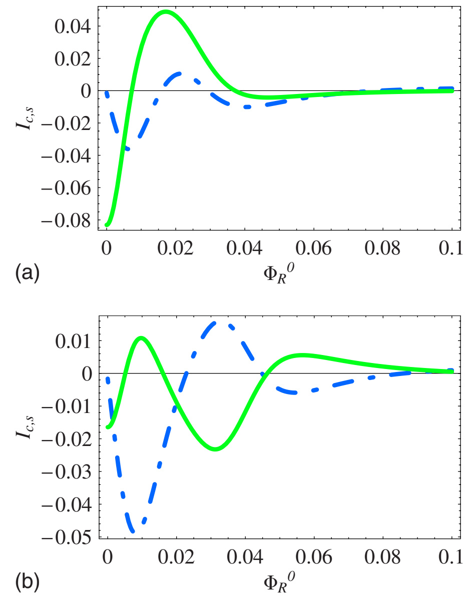

FIG. 5. (Color online) Charge (dashed-dotted line) and spin (full line) currents as a function of Φ_R^0 obtained for the following choice of parameters: γ=0.05, Φ_R^ω=0.01, ε_0=−0.025, ε_ω=0.05, φ=5π/4, ω=0.3, U=0.02, Φ_{AB}=0.49 in the upper panel, and Φ_{AB}=0.52 in the lower panel.

value. In the lower panel we set ε_ω=0, while the remaining parameters are fixed as in the upper panel. In this case the device works as a single-parameter pump associated to the Aharonov-Casher flux and the current is proportional to $(\Phi_R^\omega)^2$. A comparison between the upper and the lower panel shows that the pumping mechanism is the dominant one at

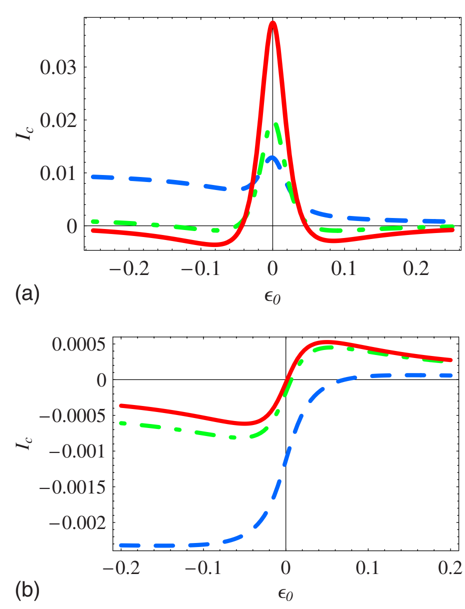

FIG. 6. (Color online) Charge current I_c as a function of ε_0 obtained for the following choice of parameters: γ=0.05, Φ_{AB}=0.49, Φ_R^0=0.05, Φ_R^ω=0.01, $\varphi=\pi/2$, U=0, ε_ω=0.05 for upper panel, and ε_ω=0 for lower panel. Each panel contains curves obtained for ω=0.1 (dashed line), ω=0.25 (dashed-dotted line), and ω=0.5 (full line).

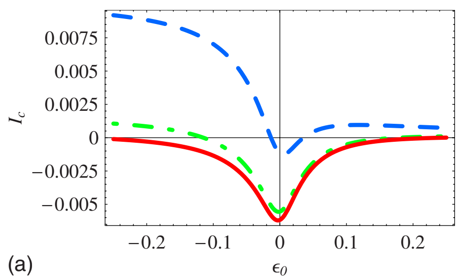

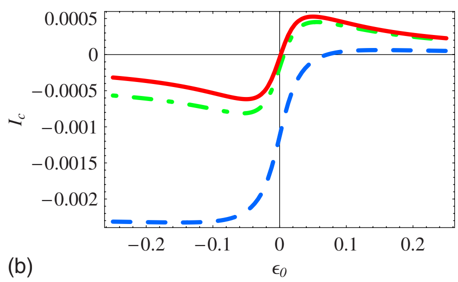

FIG. 7. (Color online) Charge current I_c as a function of ε_0 obtained for the following choice of parameters: $\gamma=0.05$, $\Phi_{AB}=0.49$, $\Phi_R^0=0.05$, $\Phi_R^\omega=0.01$, $\varphi=0$, $U=0$, $\varepsilon_\omega=0.05$ for upper panel, and $\varepsilon_\omega=0$ for lower panel. Each panel contains curves obtained for $\omega=0.1$ (dashed line), $\omega=0.25$ (dashed-dotted line), and $\omega=0.5$ (full line).

the Fermi energy. Furthermore, we have verified that a small interaction does not alter too much the picture given so far.

The same analysis performed in Fig. 6 can be repeated by setting $\varphi=0$ to include the $\cos(\varphi)$ contribution. In the upper panel of Fig. 7 we plot the current obtained for $\varepsilon_\omega=0.05$, while in the lower panel this parameter is set to zero (single-parameter pump). By comparing the results, one observes an enhancement of the absolute value of the high-frequency currents in the case of double-parameter modulation (upper panel) and close to the Fermi energy.

From the analysis above one observes that within the considered parameters region, the dominant mechanism for the generation of the dc current is the finite frequency quantum pumping. Indeed, close to the Fermi energy such currents take values which range from ~70 pA up to ~190 pA (see the upper panel of Fig. 6), while in the other cases the generated currents present values of about 10% of those induced by the pumping process. Thus, for Φ_{AB} close to half-integer values the quantum pumping induces the main contribution to the current, while away from this flux region the rectification currents are dominant.

V. CONCLUSIONS

We studied the time-dependent charge and spin transport (pumping) in a Aharonov-Bohm-Casher ring sequentially coupled to a weakly interacting quantum dot by using a nonequilibrium Green's-function approach. By varying a considerable number of parameters, we showed that the proposed device can work as a spin current generator and analyzed all its characteristics, including rectification effects. When the energy level $\varepsilon(t)$ on the dot and the Aharonov-Casher flux are periodically modulated in time with a frequency ω, a dc current is observed in the leads. Contrarily to the adiabatic case, the current-phase relation presents two additional cosine terms. The first one comes from the interaction on the dot, while the second can be interpreted as a rectification effect, as already noted in Ref. 24. We also showed that Coulomb interaction effects can enhance the rectification effects. As a function of the spin-orbit interaction and close to the nonadiabatic regime, the results of the charge current show the appearance of additional zeros at varying the Aharonov-Casher flux. Thus, the finite frequency regime close to 750 MHz ($\omega=0.3$) is suitable to obtain pure spin currents useful in spintronics. Such currents are of the order of magnitude of ~100 pA as detected in the experiments on quantum dots.[27] Finally, the analysis as a function of the dot level showed a characteristic asymmetric behavior and the comparison between the single-parameter and double-parameters pumps showed a considerable increase in the dc current in the second case. The proposed device can be easily fabricated on a GaAs/AlGaAs two-dimensional electron gas using electron-beam (e-beam) lithography to define the ring and dot region modifying, for instance, the system studied in Ref. 27.

[1] R. Hanson, L. P. Kouwenhoven, J. R. Petta, S. Tarucha, and L. M. K. Vandersypen, Rev. Mod. Phys. **79**, 1217 (2007).
[2] *Semiconductor Spintronics and Quantum Computation*, edited by D. D. Awschalom, D. Loss, and N. Samarth (Springer, Berlin, 2002).
[3] I. Žutić, J. Fabian, and S. D. Sarma, Rev. Mod. Phys. **76**, 323 (2004).
[4] Y. Aharonov and A. Casher, Phys. Rev. Lett. **53**, 319 (1984).
[5] E. I. Rashba, Sov. Phys. Solid State **2**, 1109 (1960).
[6] Y. A. Bychkov and E. I. Rashba, J. Phys. C **17**, 6039 (1984).
[7] Y. Aharonov and D. Bohm, Phys. Rev. **115**, 485 (1959).
[8] J. Splettstoesser, M. Governale, and U. Zülicke, Phys. Rev. B **68**, 165341 (2003).
[9] D. Frustaglia, M. Hentschel, and K. Richter, Phys. Rev. B **69**, 155327 (2004).
[10] D. J. Thouless, Phys. Rev. B **27**, 6083 (1983).
[11] P. W. Brouwer, Phys. Rev. B **58**, R10135 (1998).
[12] M. Switkes, C. M. Marcus, K. Campman, and A. C. Gossard, Science **283**, 1905 (1999).
[13] P. W. Brouwer, Phys. Rev. B **63**, 121303(R) (2001).
[14] B. Wang, J. Wang, and H. Guo, Phys. Rev. B **65**, 073306 (2002).
[15] J. Nitta, T. Akazaki, H. Takayanagi, and T. Enoki, Phys. Rev. Lett. **78**, 1335 (1997).
[16] R. Citro and F. Romeo, Phys. Rev. B **77**, 193309 (2008).
[17] M. Abramowitz and I. A. Stegun, *Handbook of Mathematical Functions with Formulas, Graphs, and Mathematical Tables* (Dover Publications, New York, 1972).
[18] A. P. Jauho, N. S. Wingreen, and Y. Meir, Phys. Rev. B **50**, 5528

(1994).

[19] The two-time Fourier transform has been defined according to the following relations. $g(t_1,t_2)=\int\frac{dE_1}{2\pi}\frac{dE_2}{2\pi}g(E_1,E_2)\exp\{-iE_1t_1+iE_2t_2\}$ and $g(E_1,E_2)=\int dt_1dt_2g(t_1,t_2)\exp\{iE_1t_1-iE_2t_2\}$.

[20] D. C. Langreth and P. Nordlander, Phys. Rev. B **43**, 2541 (1991).

[21] J. Splettstoesser, M. Governale, J. König, and R. Fazio, Phys. Rev. Lett. **95**, 246803 (2005).

[22] H. Bruus and K. Flensberg, *Many Body Quantum Theory in Condensed Matter Physics: An Introduction* (Oxford University Press, Oxford, 2004).

[23] S. Doniach and E. H. Sondheimer, *Green's Functions for Solid State Physicists* (Imperial College, London, 2004).

[24] L. Di Carlo, C. M. Marcus, and J. S. Harris, Jr., Phys. Rev. Lett. **91**, 246804 (2003).

[25] R. Citro and F. Romeo, Phys. Rev. B **73**, 233304 (2006).

[26] M. Braun and G. Burkard, Phys. Rev. Lett. **101**, 036802 (2008).

[27] S. K. Watson, R. M. Potok, C. M. Marcus, and V. Umansky, Phys. Rev. Lett. **91**, 258301 (2003).